Geophysical Research Letters

RESEARCH LETTER
10.1029/2025GL118494

Uncertainty in El Niño-Driven Northwest Pacific Anticyclone Projections Linked to Indo-Pacific Circulation Changes

Wenping Jiang[1,2,3], Ping Huang[4,5], Jin-Yi Yu[3], Xiangzhou Song[1,2], Mengyan Chen[6], and Gang Huang[4,7]

[1]Key Laboratory of Marine Hazards Forecasting, Ministry of Natural Resources (MNR), Hohai University, Nanjing, China, [2]College of Oceanography, Hohai University, Nanjing, China, [3]Department of Earth System Science, University of California, Irvine, CA, USA, [4]National Key Laboratory of Earth System Numerical Modeling and Application, Institute of Atmospheric Physics, Chinese Academy of Sciences, Beijing, China, [5]Center for Monsoon System Research, Institute of Atmospheric Physics, Chinese Academy of Sciences, Beijing, China, [6]State Key Laboratory of Tropical Oceanography, South China Sea Institute of Oceanology, Chinese Academy of Sciences, Guangzhou, China, [7]University of Chinese Academy of Sciences, Beijing, China

Abstract The Northwest Pacific anomalous anticyclone (NWPAC) links El Niño to East Asian summer climate, yet its response to global warming remains highly uncertain. Analyzing 48 CMIP5/6 models, this study identifies projected changes in Indo-Pacific climatological circulation as key drivers of this uncertainty. Models with a stronger weakening of the Indo-Pacific Walker circulation project deeper thermoclines in the southwest and shallower ones in the subtropical south Indian Ocean, along with a faster ENSO decay. These changes enhance Indian Ocean SST anomalies and strengthen the NWPAC through adjustments in thermocline–SST coupling and Indo-Pacific air–sea interactions. In contrast, models with weaker circulation changes project reduced Indian Ocean SST anomaly warming and a weaker NWPAC. These findings highlight the Indo-Pacific climatological wind changes, acting through thermocline–SST coupling and cross-basin air-sea interactions, play a critical role in driving intermodel uncertainty in projections of NWPAC and East Asian climate under global warming.

Plain Language Summary Summer climate over East Asia is strongly influenced by the Northwest Pacific anomalous anticyclone (NWPAC) associated with El Niño events. Understanding how this anticyclone responds to global warming is key to predicting future climate risks such as floods and heatwaves. However, current climate models exhibit substantial uncertainty in their projections. This study reveals that a major source of this uncertainty stems from how models project changes in climatological circulations over the Indo-Pacific. These circulations modulate a series of air-sea interactions in the tropical Indian Ocean, which in turn shape the response of the NWPAC during El Niño decay summers under global warming. Models projecting a stronger weakening of climatological Indo-Pacific Walker circulations tend to project a stronger NWPAC, while those with weaker changes project a weaker NWPAC. These findings reveal that how well we project Indo-Pacific states crucially affects the reliability of future summer climate projections in East Asia.

Key Points:

- The El Niño-related Northwest Pacific anomalous anticyclone (NWPAC) responds differently to global warming due to varied tropical Indian Ocean circulation projections
- Models with a stronger (weaker) decrease in Indo-Pacific circulation tend to predict a stronger (weaker) NWPAC in a future warming world
- The study underscores the key role of wind–thermocline–sea surface temperature anomaly coupling and cross-basin air-sea interactions in shaping future NWPAC changes

Supporting Information:

Supporting Information may be found in the online version of this article.

Correspondence to:

W. Jiang,
jiangwenping@hhu.edu.cn

Citation:

Jiang, W., Huang, P., Yu, J.-Y., Song, X., Chen, M., & Huang, G. (2025). Uncertainty in El Niño-driven Northwest Pacific anticyclone projections linked to Indo-Pacific circulation changes. *Geophysical Research Letters*, *52*, e2025GL118494. https://doi.org/10.1029/2025GL118494

Received 4 AUG 2025
Accepted 10 NOV 2025

Author Contributions:

Conceptualization: Wenping Jiang, Ping Huang, Jin-Yi Yu
Formal analysis: Wenping Jiang
Funding acquisition: Wenping Jiang, Xiangzhou Song
Supervision: Jin-Yi Yu
Validation: Wenping Jiang
Writing – original draft: Wenping Jiang
Writing – review & editing: Ping Huang, Jin-Yi Yu, Xiangzhou Song, Mengyan Chen, Gang Huang

1. Introduction

The Northwest Pacific anomalous anticyclone (NWPAC), driven by El Niño events, plays a critical role in shaping East Asia's summer climate (M. Y. Chen et al., 2019; Chou et al., 2003; Hu et al., 2014; Lau & Nath, 2000; B. Wang et al., 2000, 2003; Zhang & Sumi, 2002; Zhang et al., 1999). It is a local ocean–atmosphere coupling mode that can be generated by multiple factors (Fan et al., 2013; Lu et al., 2023; B. Wang et al., 2000; G. Wang et al., 2020; Xie et al., 2009), and here we focus on the component forced by ENSO, which typically initiates during the El Niño developing autumn, strengthens during the El Niño mature winter, and persists through the subsequent spring and summer (B. Wang et al., 2000; B. Wu et al., 2017; Zhang et al., 1996). By modulating the Western Pacific Subtropical High, the NWPAC significantly influences rainfall, temperature anomalies in East Asia, and tropical cyclone activities over the Northwest Pacific (NWP) (Cao et al., 2018; Liu & Chen, 2018; B. Wang et al., 2013; G. Wang et al., 2020; Zhao & Wang, 2019), often leading to floods, droughts, and heatwaves (Chang et al., 2000; B. Wang et al., 2000; Zhang et al., 2017).

Several mechanisms explain how ENSO, despite peaking in winter, influences the NWPAC into the following summer, largely through sea surface temperature anomalies (SSTAs) across multiple ocean basins. In the NWP, El Niño-induced local cold SSTAs help sustain the NWPAC via positive local air–sea feedback from boreal winter through early summer (B. Wang et al., 2000, 2003; B. Wu et al., 2010). Concurrently, El Niño-driven warming in the tropical Indian Ocean (TIO) can excite an eastward-propagating atmospheric Kelvin wave that suppresses convection over the western Pacific, maintaining the NWPAC via Ekman divergence (Xie et al., 2009; Yang et al., 2007, 2010). A cross-basin coupled mode integrating both the NWP and TIO mechanisms has also been identified (Xie et al., 2016). Additionally, previous studies have suggested that cold SSTAs emerge in the equatorial western Pacific (EWP) during fast-decaying El Niño summers, which may trigger a Gill-type Rossby wave response that enhances the NWPAC (Fan et al., 2013; W. Jiang et al., 2019).

Given rising greenhouse gas emissions, understanding the response of El Niño-related NWPAC to global warming is critical for projecting future East Asian climate variability. However, projections remain inconclusive (He & Zhou, 2022; He et al., 2019; Hu et al., 2014; W. Jiang et al., 2018; Tao et al., 2015; Zheng et al., 2011). Existing studies offer divergent perspectives. Some studies find little anthropogenic influence, suggesting that the decadal modulation of NWPAC variability is primarily driven by natural climate variability such as the PDO or AMO (Chowdary et al., 2012; Song & Zhou, 2015), while others find anthropogenic forcing either strengthens (W. Chen et al., 2016; Hu et al., 2014; Tao et al., 2015; Zheng et al., 2011) or weakens the NWPAC (He et al., 2019; W. Jiang et al., 2018). CMIP5 and CMIP6 models even yield opposite projections (He & Zhou, 2022). These discrepancies underscore substantial uncertainties in projecting the El Niño–related NWPAC response to global warming across different climate models.

Identifying the source of this uncertainty is essential for improving NWPAC projections. While previous studies have emphasized the role of El Niño forcing itself (M. Wu et al., 2020, 2021), this study shows that projected changes in the climatological atmospheric circulation over the TIO represent a more influential yet underexplored driver. We demonstrate that intermodel divergence in TIO circulation modulates the NWPAC through its impact on thermocline depth and SST in the southwest and subtropical southern Indian Ocean. These results underscore the importance of improving the simulation of TIO mean-state changes to reduce uncertainty in future projections of the Asian summer climate.

2. Methods and Data

Unlike our previous work that selected models with realistic NWPAC simulations to investigate future changes in the NWPAC (W. Jiang et al., 2018), in this study, we use monthly outputs from 25 CMIP5 models (Taylor et al., 2012) and 23 CMIP6 models (Eyring et al., 2016) in historical simulations and future projections under the Representative Concentration Pathway 8.5 (RCP8.5) scenario for CMIP5 and the Shared Socioeconomic Pathway 5–8.5 (SSP5–8.5) scenario for CMIP6, respectively, in order to capture the diversity of projected NWPAC changes. The variables analyzed include monthly mean SST, oceanic potential temperature, precipitation, latent heat flux, and wind. All data sets were interpolated to a 2.5° × 2.5° horizontal resolution. A full list of models is provided in the Table S1 in Supporting Information S1. The historical period (1960–1999) is used as the present-day baseline, and 2060–2099 as the future period. Projected changes are computed as differences between these two periods and normalized by each model's global mean SST warming over 60°S–60°N to account for spread in warming magnitude.

Interannual variability signals were extracted by removing the linear trend, the annual cycle, and a 13-year running mean from the original data sets. ENSO-related variability is denoted by regressing anomalies of variables onto the unstandardized Niño-3.4 index (December-January-February SSTAs averaged over 5°S–5°N, 120°W–170°W), which quantifies responses per 1 K Niño-3.4 SST anomaly. This method, widely used in previous studies (e.g., W. Jiang et al., 2018; M. Wu et al., 2020), minimizes the influence of intermodel uncertainty of ENSO amplitude changes. We focus on the influence of projected ENSO pattern and precipitation changes on the NWPAC and on the factors contributing to their projection uncertainty. The El Niño-related NWPAC change index is defined as the ENSO-related change in 850-hPa relative vorticity over the NWP (10°N–30°N, 90°E–180°E) during June–July–August (JJA) of the year following the ENSO peak. Thermocline depth is defined as the depth of the maximum vertical gradient in temperature.

To evaluate the contribution of wind speed to latent heat flux variations, we follow Du and Xie (2008) and express the wind speed-induced component in a linear form:

$$Q'_{EW} = \overline{Q_E}\frac{W'}{\overline{W}},$$

where Q'_{EW} denotes wind speed-related latent heat flux anomalies, $\overline{Q_E}$ is climatological latent heat flux. W' is wind speed anomalies and $\overline{W}$ represents climatological wind speed. This term is commonly regarded as the wind–evaporation–SST (WES) feedback.

The statistical significance of the correlation coefficients is assessed using a two-tailed Student's *t*-test. The intermodel consensus is defined as the percentage of models that agree with the MME on the sign of change. Following Power et al. (2012), a 68% consensus is considered statistically robust, corresponding to the 95% confidence level assuming models independence.

3. Results

3.1. Large Intermodel Uncertainty in Projecting NWPAC Changes and Its Primary Source

To examine intermodel uncertainty in projected changes of the El Niño–related NWPAC during the decaying summer, we performed an intermodel empirical orthogonal function (EOF) analysis of ENSO-related 850-hPa relative vorticity changes over the NWP (10°N–30°N, 90°E–180°E) for June-July-August of the decaying year [JJA(1)]. Here, the notation "(1)" refers to calendar months in the decaying year of El Niño, while "(0)" denotes the developing year. The leading intermodel EOF mode (EOF1), shown in Figure 1a, accounts for 31.1% of the total intermodel variance and reveals that the primary uncertainty in NWPAC projections manifests as a meridional dipole pattern over the NWP and EWP regions. The largest uncertainty is centered over the NWP, as indicated by substantial intermodel standard deviations in JJA(1) ENSO-related 850-hPa relative vorticity changes. The corresponding principal component (PC1), shown in Figure 1b, effectively discriminates model behaviors: models with positive PC1 values tend to project an intensified NWPAC during post-El Niño summer under global warming, whereas models with negative PC1 values tend to project a weakened response. The intermodel correlation coefficient between the NWPAC changes index and PC1 is 0.96 (Figure 1c), indicating that the EOF1 robustly captures the primary characteristics of intermodel uncertainty in projections of El Niño–related NWPAC changes. EOF2 explains 17.7% of the total intermodel variance but its principal component shows only a weak and insignificant correlation with the NWPAC change index ($r = -0.12$, Figure S1 in Supporting Information S1), indicating that higher-order modes do not effectively represent the intermodel spread of NWPAC changes. An EOF analysis using 850-hPa geopotential height gives similar but weaker correlation with the NWPAC change (Figure S2 in Supporting Information S1), therefore, we base our analysis on the vorticity-derived EOF following M. Wu et al. (2020).

Based on the normalized PC1 values, we select 11 models with PC1 larger than 0.6 (Group A; model names listed in Table S1 in Supporting Information S1) and 11 models with PC1 less than −0.6 (Group B; same as above) for composite analysis. Group A projects a stronger NWPAC in a warmer world, while Group B projects a weaker NWPAC. We mainly focus on these two groups to explore the sources of intermodel uncertainty in projecting NWPAC changes by comparing their differences. Figure 2 shows the ENSO-related SST and 850-hPa wind anomalies in the two model groups and their differences. Figures S3 and S4 in Supporting Information S1 further present the ENSO-related SST and wind anomalies in historical simulations and future warming scenarios. In historical simulations, ENSO peaks during the mature winter and decays in the following spring and summer in both groups (Figures S3a–S3c and S4a–S4c in Supporting Information S1). The NWPAC develops in the mature winter, strengthens in spring, and persists until the decaying summer in both groups (Figures S3a–S3c and S4a–S4c in Supporting Information S1). Notably, both groups exhibit a common bias—an excessive westward extension and slow decay of ENSO-related SSTAs, largely attributed to the excessively strong and westward extended cold tongue in the equatorial Pacific (W. Jiang et al., 2017, 2021).

Under global warming, the transition from El Niño to La Niña accelerates compared to the historical period in Group A and Group B (Figures S3d–S3f in Supporting Information S1), whereas this acceleration is relatively modest in Group B (Figures S4d–S4f in Supporting Information S1). This difference is reflected in the larger sea surface temperature anomaly (SSTA) changes over the equatorial western and central Pacific in Group A than in Group B between the two periods (Figures 2g–2i). The contrasting changes in ENSO decay pace are further confirmed by the evolution of the Niño3.4 index between historical simulations and warming projections for the

10.1029/2025GL118494

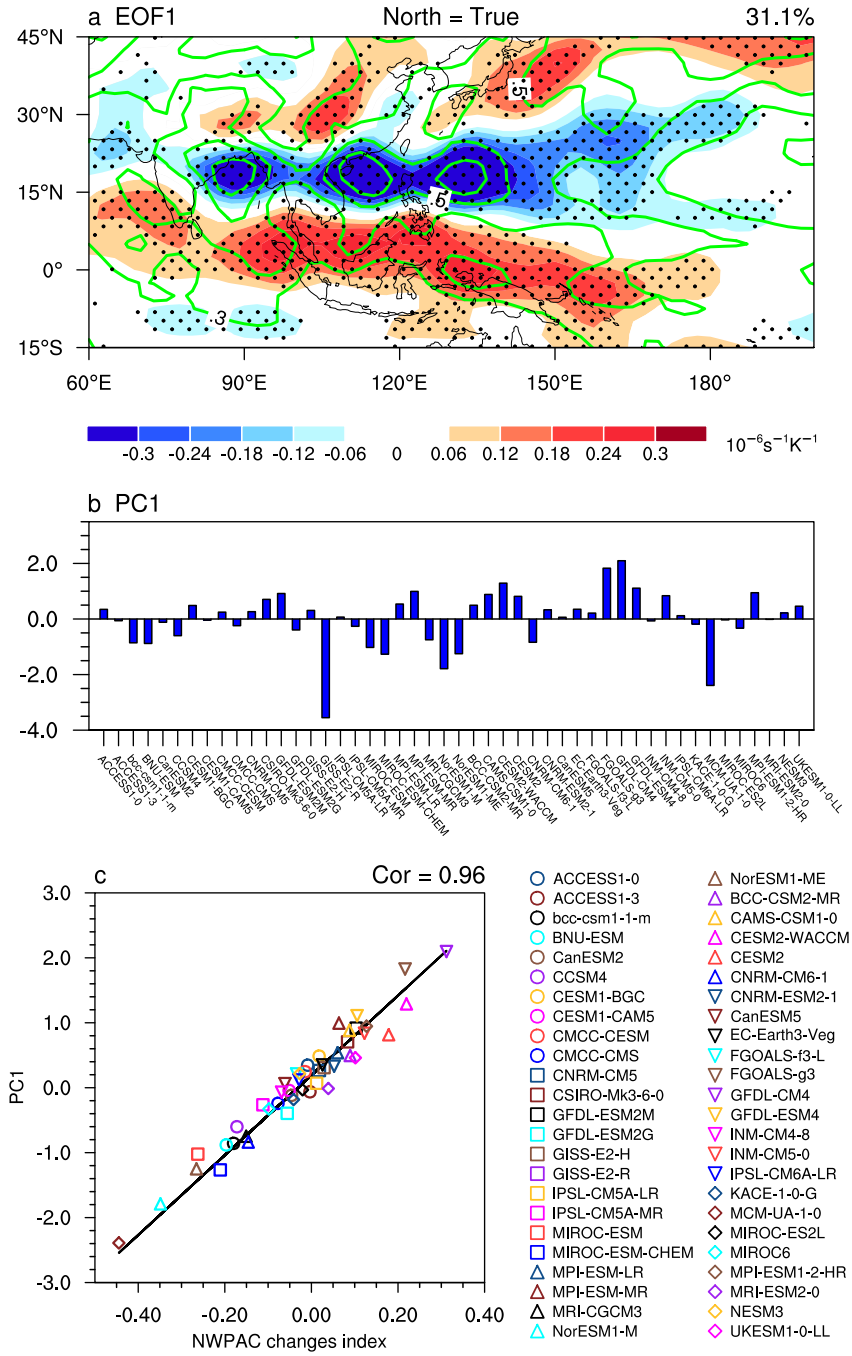

Figure 1. Leading mode (EOF1) of intermodal spread in projected Northwest Pacific anomalous anticyclone (NWPAC) changes. (a) EOF1 of projected JJA(1) changes in 850-hPa relative vorticity (shading, units: 10^{-6} s^{-1} K^{-1}) during 2060–2099 relative to 1960–1999, with intermodel standard deviation (contours; units: 1). The explained variance is given at top-right, and North's test result (North = True) indicates that EOF1 is statistically separable from adjacent modes. (b) The corresponding PC1 values for each model. (c) Scatterplot of PC1 versus the NWPAC change index in JJA(1) across the 48 models. The correlation coefficient (shown in the top-right) is significant at the 99% confidence level through the Student's *t*-test.

two groups (Figure S5 in Supporting Information S1). Figures 2c and 2f also show that the NWPAC is projected to strengthen from the historical experiments to future warming scenarios in Group A, but to weaken in Group B. These intermodel differences highlight a close linkage between the ENSO decay pace and NWPAC intensity

10.1029/2025GL118494

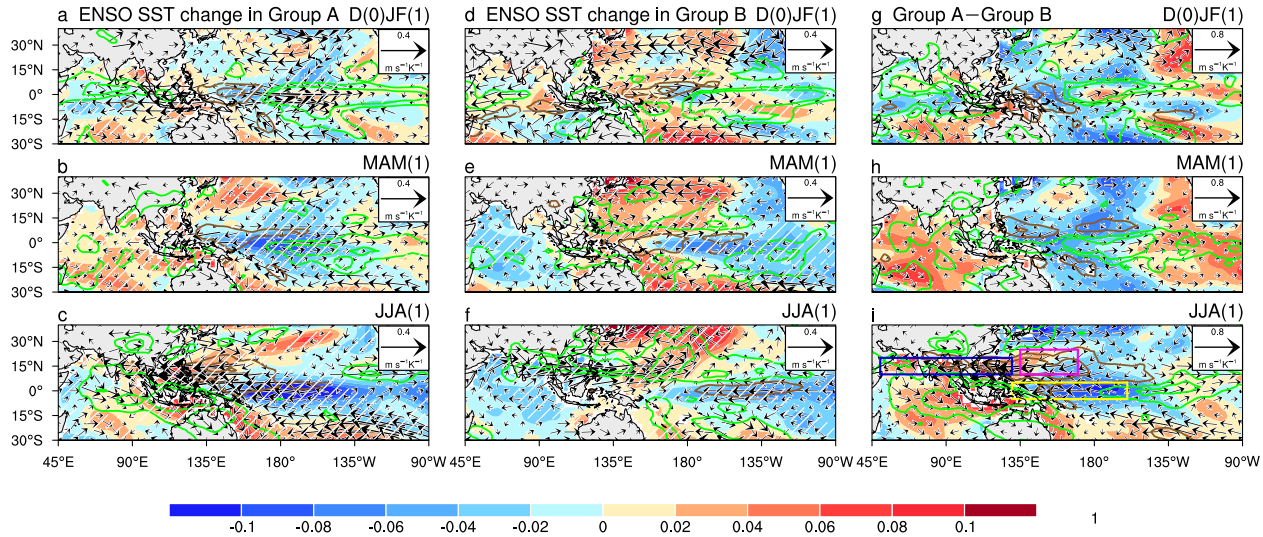

Figure 2. Changes in ENSO-related anomalies between two groups and their differences. SST (shadings, 1), precipitation (contours, mm day^{-1} K^{-1}) and 850-hPa wind (vectors, m s^{-1} K^{-1}) anomalies during D(0)JF(1) to JJA(1) for (a–c) the historical period, (d–f) RCP8.5/SSP5-8.5 scenarios, and (g–i) their difference. Green and brown contours denote precipitation anomalies of ±0.2 and ±0.4 mm day^{-1} K^{-1}. Stippled regions in panels (a–f) indicate the regions where the sign of the MME agrees in more than 68% of models. Blue, yellow, and magenta boxes in panel (i) mark the tropical Indian Ocean, equatorial western Pacific, and Northwest Pacific regions, respectively.

under global warming, consistent with M. Wu et al. (2020), who reported that models projecting a faster ENSO decay tend to project a stronger NWPAC owing to cold SSTAs in the EWP.

Notably, the differences in ENSO-related SSTA changes between the two groups are also pronounced in the TIO. In Group A, the subtropical south Indian Ocean (SSIO) exhibits warmer ENSO-related SSTAs during the mature winter in a warmer world (Figure 2a), which extend into the TIO in the following spring (Figure 2b). During the decaying summer, stronger SSTA warming occurs in the north and east TIO and the local NWP (Figure 2c). In contrast, Group B displays nearly opposite SSTA changes in the Indian Ocean (Figures 2d–2f). These contrasting SSTA responses constitute the dominant features of the projected differences in Indian Ocean SSTAs between the two model groups (Figures 2g–2i). Previous studies have shown that warmer SSTAs in the TIO, along with cooler SSTAs in the local NWP and EWP, contribute to strengthening the NWPAC during post-El Niño summer (Fan et al., 2013; W. Jiang et al., 2019; B. Wang et al., 2000; Xie et al., 2009). Moreover, Xie et al. (2016) proposed the Indo-Pacific Ocean Capacitor mechanism, highlighting the cross-basin coupling processes whereby SSTAs in the TIO and the western Pacific can sustain and feedback onto the NWPAC. Therefore, intermodel differences in the projected ENSO-related SSTAs across multiple ocean basins likely underlie the uncertainty in NWPAC projections through ocean–atmosphere interactions.

To identify the dominant SSTA sources of intermodel uncertainty in projecting NWPAC changes, Figure 3 presents the relationships between PC1 and SSTA changes in the TIO, EWP, and the local NWP. Among the 48 CMIP models analyzed, the correlation coefficients between NWPAC changes and projected SSTA changes in the north Indian Ocean (NIO; 10°N–20°N, 50°E–130°E, blue box in Figure 2i), EWP (5°S–5°N, 130°E–160°W, yellow box in Figure 2i), and NWP (10°N–25°N, 135°E–170°E, magenta box in Figure 2i) are 0.75, −0.56, and −0.16, respectively (Figure 3). Among the three regions analyzed, the correlation between local NWP SSTA and NWPAC changes is weak and not statistically significant. In contrast, the TIO exhibits the strongest relationship with NWPAC changes, significant at the 99% confidence level. The EWP also shows a statistically significant correlation at the 99% level, though its influence is weaker than that of the TIO. These findings indicate that although both warmer TIO SSTA and colder EWP SSTA changes contribute to strengthening the NWPAC in CMIP models, the dominant contribution to intermodel uncertainty in future NWPAC projections stems from the large uncertainty in projected TIO SSTA changes. This conclusion remains robust when accounting for ENSO amplitude changes by regressing variables onto the standardized Niño-3.4 index (Figure S6 in Supporting Information S1).

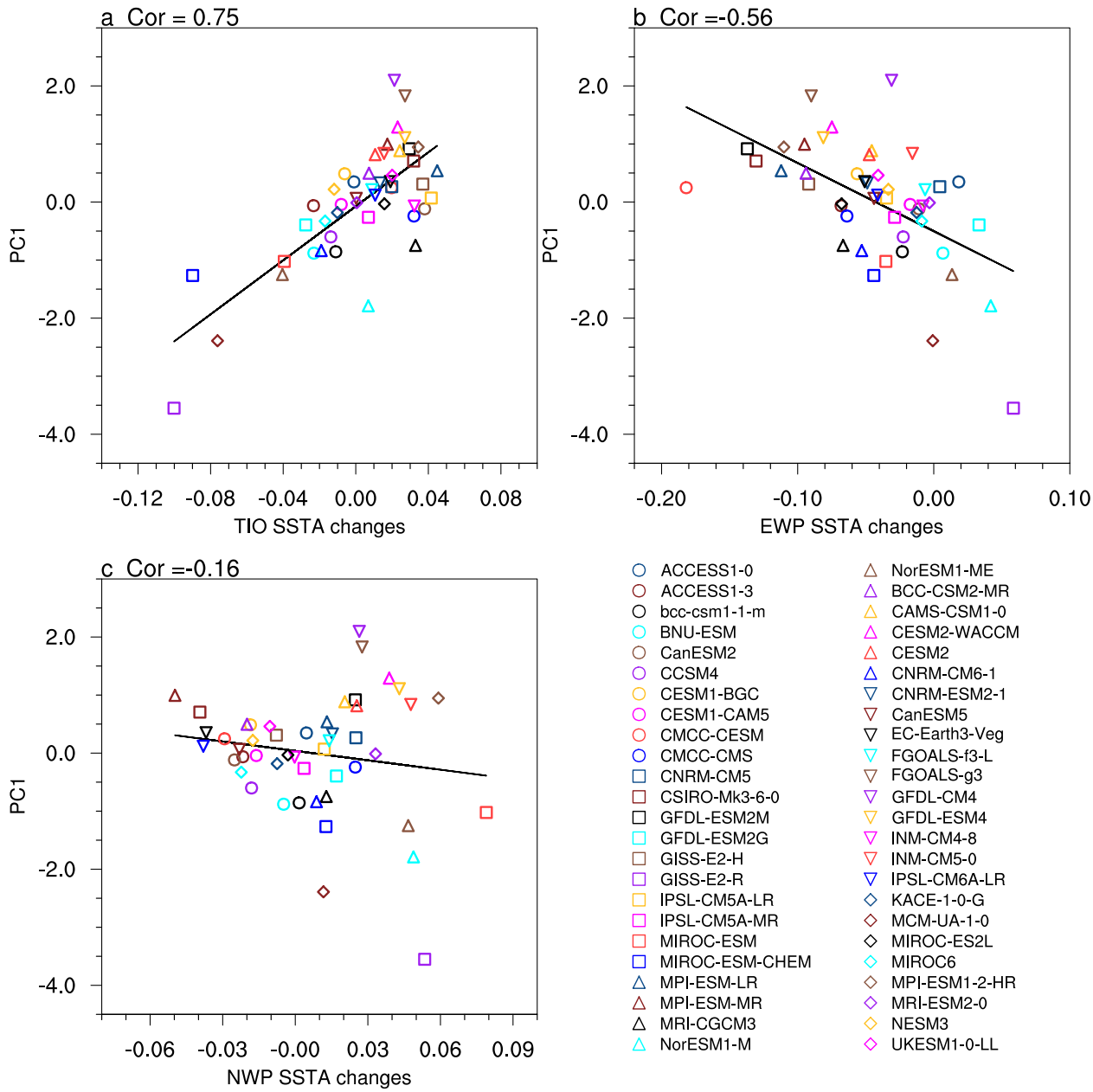

Figure 3. Statistical relationships between PC1 and tropical Indian Ocean (TIO)/equatorial western Pacific (EWP)/Northwest Pacific (NWP) sea surface temperature anomalie (SSTA) changes. Scatterplots of the PC1 versus (a) TIO SSTA changes, (b) EWP SSTA changes, and (c) NWP SSTA changes. The black lines denote the linear fit between the horizontal and vertical coordinates in 48 models. The intermodel correlation coefficients are shown at the top left of the panels.

3.2. Mechanisms Behind Intermodel Diversity in Projected TIO SSTA Changes and Their Influence on El Niño-Driven NWPAC

As shown in Figure 2, the two model groups exhibit contrasting ENSO-induced SSTA evolutions in the TIO, particularly in the SSIO and northern TIO during post-El Niño summers. In Group A, warm SSTAs develop in the SSIO during the El Niño mature winter and progressively extend northward and eastward into the broader TIO. In contrast, Group B displays much weaker warming or even cold anomalies. These distinct seasonal SSTA patterns suggest that intermodel differences in TIO warming may arise from processes that propagate or amplify anomalies across the basin. We next examine the mechanisms responsible for these divergent responses, focusing on oceanic wave dynamics and local air-sea feedback.

10.1029/2025GL118494

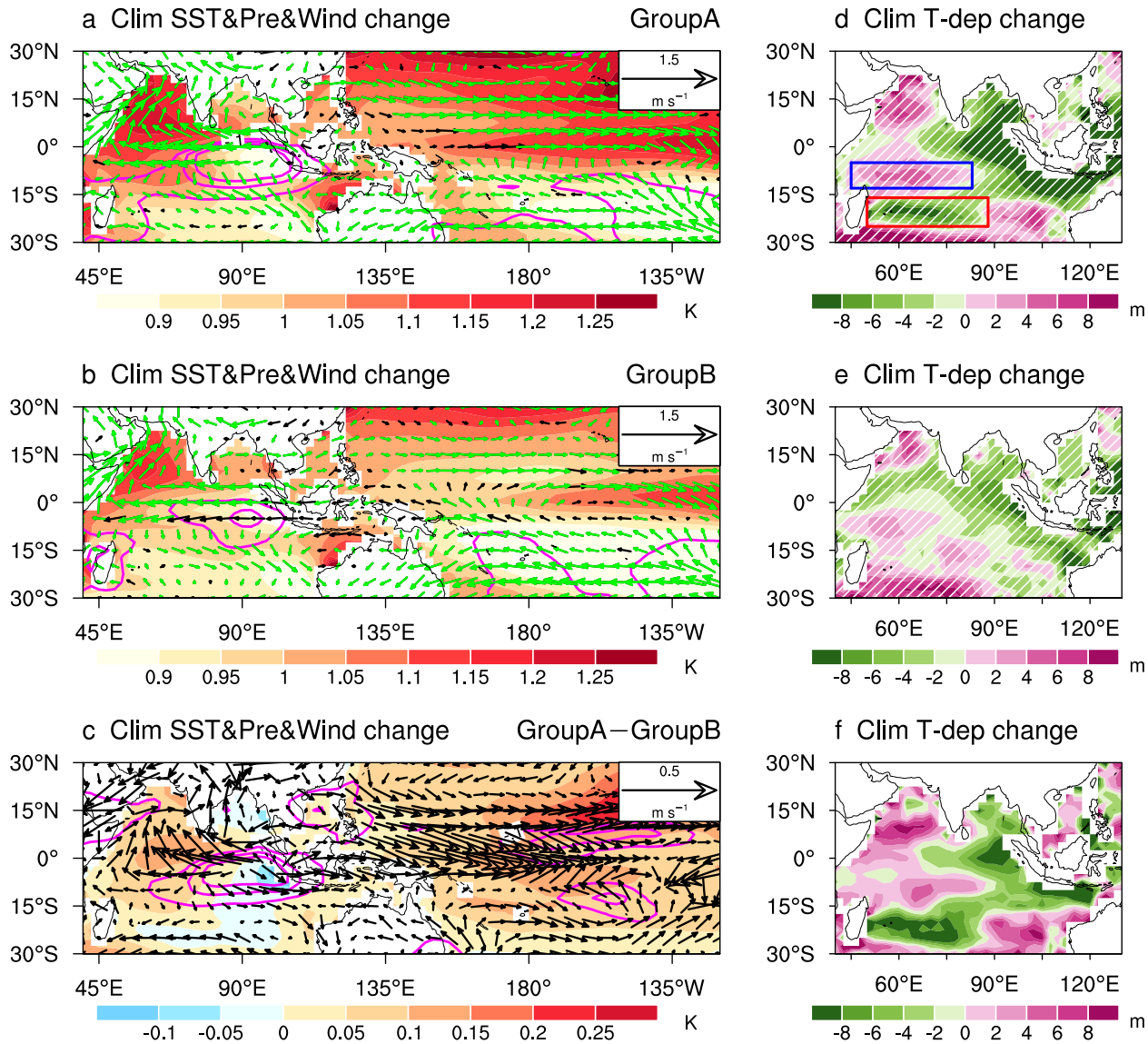

Figure 4. Changes from historical to future warming simulations in climatological SST (shading, K), precipitation (magenta contours at −0.5, −0.3, and −0.1 mm day^{-1}) and 850-hPa winds (vectors, m s^{-1}) during SON for (a) Group A, (b) Group B, and (c) their difference. (d–f) Same as (a–c) but for thermocline depth (shading, m) during DJF. Green vectors in panels (a, b) and stippling in panels (d, e) indicate >68% model agreement on MME sign. Blue and red boxes mark the southwestern tropical Indian Ocean and subtropical south Indian Ocean, respectively.

To identify sources of intermodel uncertainty in projected TIO SSTA changes, Figure 4 compares historical-to-future changes in climatological winds, precipitation, SST during boreal autumn, and thermocline depth during boreal winter for two Groups. Both groups project an El Niño–like mean-state SST warming and a weakened Walker circulation across the Indo-Pacific (Figures 4a and 4b). The Pacific and Indian Ocean Walker circulations vary coherently, as both are regulated by convection anchored in the warm pool (Han et al., 2025).

In the Pacific, a weakened and eastward-shifted Walker circulation strengthens wind divergence and latent-heat damping over the EWP, accelerating ENSO decay (Lin et al., 2024). Group A projects stronger weakening of the Pacific Walker circulation (Figures 4a and 4c), faster ENSO decay (Figure S5 in Supporting Information S1), and stronger suppressed EWP convection during D(0)JF(1) (Figure 2a), while Group B shows weaker weakening of the Pacific Walker circulation (Figures 4b and 4c), a relatively modest ENSO decay (Figure S5 in Supporting Information S1), and even enhanced Maritime Continent convection anomalies (Figure 2d). Consequently, the suppressed convection changes in Group A excite a pair of anticyclonic anomalies over the SSIO and NWP

through triggering a Gill-type response, whereas enhanced convection changes in Group B excite cyclonic anomalies (Figures 2a and 2d). In Group A, the strengthened NWPAC in turn accelerates ENSO decay, establishing a positive feedback between EWP SSTA and NWPAC changes.

In the Indian Ocean, the weakened Walker circulation suppresses convection over the eastern TIO–Maritime Continent and induces a Gill–type anticyclonic circulation changes over the northern TIO (Gopika et al., 2025; Han et al., 2025). These winds drives northerly Ekman transport and reduced upwelling in the Arabian Sea, favoring downward Ekman pumping and thermocline deepening in the northwest TIO (Gopika et al., 2025; Sharma et al., 2023), and generate stronger westward-propagating downwelling oceanic Rossby waves, further deepening the thermocline in the southwest TIO dome (blue box in Figure 4d) (Masumoto & Meyers, 1998; Xie et al., 2002), with partial compensating shoaling in adjacent regions such as the eastern TIO and SSIO (red box in Figure 4d), possibly modulated by regional wind stress curl and other processes. Group A exhibits stronger deepening in the southwest/northwest TIO and clearer shoaling in the SSIO, whereas Group B shows weaker adjustments (Figures 4d–4f).

These climatological thermocline changes alter thermocline–SST coupling and yield distinct ENSO-related SSTA changes. In Group A, a deeper climatological thermocline in the southwest TIO increases the thermal inertia of the upper ocean, reducing the sensitivity of SST to subsurface variations. This weakens thermocline–SST coupling and suppresses ENSO-induced warm SSTAs in the southwest TIO during the El Niño mature winter (Figure 2a). This mechanism is consistent with previous studies (Li et al., 2015; Zheng et al., 2016), which suggested that a climatological easterly wind bias over the TIO can result in an overly deep mean thermocline in the southwest TIO, reducing SST variability in models. Conversely, a shallower SSIO climatological thermocline enhances ENSO-related warm SSTAs (Figure 2a). Group B, with weaker equatorial easterly changes, shows reduced thermocline deepening in the southwest TIO and weaker shoaling in the SSIO (Figure 4e). These differences in thermocline climatology between the two groups (Figure 4f) result in different ENSO-related SSIO SSTA changes (Figure 2g). Specifically, Group A projects SSTAs warming in the SSIO during the El Niño mature winter, while Group B projects SSTAs cooling (Figures 2a and 2d).

The contrasting ENSO-related SSTA changes lead to distinct local air–sea interactions, ultimately influencing projections of the future ENSO-induced NWPAC. In Group A, anticyclonic wind anomaly changes over the SSIO weaken background winds (Figure 2a and Figure S7a in Supporting Information S1), reducing latent heat flux release and favoring SSTA warming in the north TIO and SSIO in the following seasons via the WES feedback (Figure S8a in Supporting Information S1). The intensified warm SSTAs strengthen the NWPAC through an atmospheric Kelvin wave response (Xie et al., 2009; Yang et al., 2007, 2010), which is evidenced by enhanced tropospheric temperature, associated positive rainfall anomalies indicating diabatic heating over the TIO (X. Jiang et al., 2011) and 200-hPa westerly wind anomalies over the Maritime Continent (Figure S9 in Supporting Information S1). Easterlies on the southern flank of the NWPAC extend back into the Indian Ocean, further suppressing evaporation and amplifying TIO SSTA warming (Du et al., 2009; see Figure 2c and Figure S8c in Supporting Information S1). This sequence establishes a positive feedback: enhanced TIO SSTAs reinforces the NWPAC, which in turn promotes additional SSTAs warming. In Group B, cyclonic wind anomalies over the SSIO enhance latent heat flux release, reducing SSTA changes that extend from the SSIO to the north TIO (Figures 2d–2f and Figures S8d–S8f in Supporting Information S1), ultimately weakening the NWPAC. Additional analyses shows that longwave radiation and sensible heat fluxes contribute little, while shortwave radiation has a positive effect over the north TIO but a negative effect across most of the basin (Figure S10 in Supporting Information S1).

4. Conclusion and Discussion

Projections of El Niño-related NWPAC changes under global warming exhibit large intermodel uncertainty. Using outputs from 25 CMIP5 and 23 CMIP6 models, this study identifies the dominant source of this uncertainty arising from Indo-Pacific Walker circulation changes. On the one hand, weakening of the Indian Ocean Walker circulation alters thermocline depth in the southwest TIO and SSIO, thereby modifying ENSO-related TIO SSTAs via thermocline–SST coupling. On the other hand, a weakened Pacific Walker circulation accelerates ENSO decay, leading to earlier cold SSTAs in the EWP. These changes affect atmospheric convection over the Maritime Continent and induce divergent circulation anomaly changes over the southern Indian Ocean, which subsequently modulate TIO SSTAs changes via the WES feedback. Together, these processes shape different TIO

SSTAs changes across models and ultimately control the intermodel uncertainty in NWPAC projections during the post-El Niño summer.

Previous studies have identified the El Niño decay pace as a major source of uncertainty in NWPAC projections (L. Wang et al., 2025; M. Wu et al., 2020, 2021). Our study confirms this role but further reveals that intermodel differences in the projected Indo-Pacific Walker circulation constitute an additional and less explored driver of uncertainty. In particular, the changes in background winds alter climatological thermocline depth, circulation anomalies and SSTA responses in the SSIO during ENSO mature winters, which emerge as critical modulators of ENSO-related TIO SSTA changes in subsequent seasons. This new finding underscores that NWPAC projections uncertainty is shaped not only by ENSO decay pace but also by Indo-Pacific mean-state circulation changes. Together, these results highlight the importance of improving projection of Indian Ocean mean-state and their coupling with cross-basin processes, providing new avenues for reducing uncertainty in projections of the Asian summer climate.

While no systematic resolution differences were found between Groups A and B, other technical aspects such as coupling strategies, parameterization schemes, or mean state biases may still contribute to divergent projections of ENSO-related SSTAs and NWP circulation changes. Although a comprehensive diagnosis of these factors is beyond the scope of this study, future work on model formulation and air–sea coupling could provide further insights into the origins of intermodel spread.

Conflict of Interest

The authors declare no conflicts of interest relevant to this study.

Data Availability Statement

The CMIP5 model data (Taylor et al., 2012) and CMIP6 model data (Eyring et al., 2016) used in this study are publicly available from the CMIP data portals. The codes used for the main analysis are available via W. Jiang et al. (2025).

Acknowledgments
We thank the modeling groups for producing and making available their CMIP5/CMIP6 outputs. This work complies with the AGU Data Policy: all data and methods used in this study are publicly available. This study is supported by the National Natural Science Foundation of China projects (Grants 42476017, 42141019, 42425601, and 42005022). We acknowledge the constructive comments and suggestions from the anonymous reviewers.

References

Cao, X., Wu, R., & Xiao, X. (2018). A new perspective of intensified impact of El Niño-Southern Oscillation Modoki on tropical cyclogenesis over the western North Pacific around 1990s. *International Journal of Climatology*, *38*(11), 4262–4275. https://doi.org/10.1002/joc.5667

Chang, C. P., Zhang, Y. S., & Li, T. (2000). Interannual and interdecadal variations of the East Asian summer monsoon and tropical Pacific SSTs. Part I: Roles of the subtropical ridge. *Journal of Climate*, *13*(24), 4310–4325. https://doi.org/10.1175/1520-0442(2000)013<4310:IAIVOT>2.0.CO;2

Chen, M. Y., Yu, J. Y., Wang, X., & Jiang, W. (2019). The changing impact mechanisms of a diverse El Niño on the Western Pacific subtropical high. *Geophysical Research Letters*, *46*(2), 953–962. https://doi.org/10.1029/2018GL081131

Chen, W., Lee, J.-Y., Ha, K.-J., Yun, K.-S., & Lu, R. (2016). Intensification of the Western North Pacific anticyclone response to the short decaying El Niño event due to greenhouse warming. *Journal of Climate*, *29*(10), 3607–3627. https://doi.org/10.1175/jcli-d-15-0195.1

Chou, C., Tu, J. Y., & Yu, J. Y. (2003). Interannual variability of the western North Pacific summer monsoon: Differences between ENSO and non-ENSO years. *Journal of Climate*, *16*(13), 2275–2287. https://doi.org/10.1175/2761.1

Chowdary, J. S., Xie, S. P., Tokinaga, H., Okumura, Y. M., Kubota, H., Johnson, N., & Zheng, X. T. (2012). Interdecadal variations in ENSO teleconnection to the indo-western Pacific for 1870-2007. *Journal of Climate*, *25*(5), 1722–1744. https://doi.org/10.1175/jcli-d-11-00070.1

Du, Y., & Xie, S. (2008). Role of atmospheric adjustments in the tropical Indian Ocean warming during the 20th century in climate models. *Geophysical Research Letters*, *35*(8), 2008GL033631. https://doi.org/10.1029/2008GL033631

Du, Y., Xie, S.-P., Huang, G., & Hu, K. (2009). Role of air-sea interaction in the long persistence of El Niño-induced North Indian Ocean warming. *Journal of Climate*, *22*(8), 2023–2038. https://doi.org/10.1175/2008jcli2590.1

Eyring, V., Bony, S., Meehl, G. A., Senior, C. A., Stevens, B., Stouffer, R. J., & Taylor, K. E. (2016). Overview of the Coupled Model Intercomparison Project Phase 6 (CMIP6) experimental design and organization. *Geoscientific Model Development*, *9*(5), 1937–1958. https://doi.org/10.5194/gmd-9-1937-2016

Fan, L., Shin, S. I., Liu, Q. Y., & Liu, Z. Y. (2013). Relative importance of tropical SST anomalies in forcing East Asian summer monsoon circulation. *Geophysical Research Letters*, *40*(10), 2471–2477. https://doi.org/10.1002/grl.50494

Gopika, S., Sadhvi, K., Vialard, J., Danielli, V., Neetu, S., & Lengaigne, M. (2025). Drivers of future Indian Ocean warming and its spatial pattern in CMIP models. *Earth's Future*, *13*(4), e2025EF006112. https://doi.org/10.1029/2025EF006112

Han, Z.-W., Zheng, X.-T., & Geng, Y.-F. (2025). Seasonal dependence of the projected Indian Ocean walker circulation uncertainty under greenhouse warming. *Journal of Climate*, *38*(15), 3623–3642. https://doi.org/10.1175/JCLI-D-24-0480.1

He, C., & Zhou, T. (2022). Distinct responses of North Pacific and North Atlantic summertime subtropical anticyclones to global warming. *Journal of Climate*, *35*(24), 8117–8132. https://doi.org/10.1175/JCLI-D-21-1024.1

He, C., Zhou, T., & Li, T. (2019). Weakened anomalous Western North Pacific anticyclone during an El Nino-decaying summer under a warmer climate: Dominant role of the weakened impact of the tropical Indian Ocean on the atmosphere. *Journal of Climate*, *32*(1), 213–230. https://doi.org/10.1175/jcli-d-18-0033.1

Hu, K., Huang, G., Zheng, X.-T., Xie, S.-P., Qu, X., Du, Y., & Liu, L. (2014). Interdecadal variations in ENSO influences on Northwest Pacific-East Asian early summertime climate simulated in CMIP5 models. *Journal of Climate*, *27*(15), 5982–5998. https://doi.org/10.1175/jcli-d-13-00268.1

Jiang, W., Huang, G., Hu, K., Wu, R., Gong, H., Chen, X., & Tao, W. (2017). Diverse relationship between ENSO and the Northwest Pacific summer climate among CMIP5 models: Dependence on the ENSO decay pace. *Journal of Climate*, *30*(1), 109–127. https://doi.org/10.1175/jcli-d-16-0365.1

Jiang, W., Huang, G., Huang, P., & Hu, K. (2018). Weakening of Northwest Pacific anticyclone anomalies during post-El Niño summers under global warming. *Journal of Climate*, *31*(9), 3539–3555. https://doi.org/10.1175/jcli-d-17-0613.1

Jiang, W., Huang, G., Huang, P., Wu, R., Hu, K., & Chen, W. (2019). Northwest Pacific anticyclonic anomalies during post-El Niño summers determined by the pace of El Niño decay. *Journal of Climate*, *32*(12), 3487–3503. https://doi.org/10.1175/jcli-d-18-0793.1

Jiang, W., Huang, P., Huang, G., & Ying, J. (2021). Origins of the excessive westward extension of ENSO SST simulated in CMIP5 and CMIP6 models. *Journal of Climate*, *34*(8), 2839–2851. https://doi.org/10.1175/jcli-d-20-0551.1

Jiang, W., Huang, P., Yu, J., Song, X., Chen, M., & Huang, G. (2025). Uncertainty in El Niño-driven northwest Pacific anticyclone projections linked to indo-pacific circulation changes. *Zenodo*. https://doi.org/10.5281/zenodo.17282287

Jiang, X., Waliser, D. E., Olson, W. S., Tao, W.-K., L'Ecuyer, T. S., Li, K.-F., et al. (2011). Vertical diabatic heating structure of the MJO: Intercomparison between recent reanalyses and TRMM estimates. *Monthly Weather Review*, *139*(10), 3208–3223. https://doi.org/10.1175/2011MWR3636.1

Lau, N. C., & Nath, M. J. (2000). Impact of ENSO on the variability of the Asian-Australian monsoons as simulated in GCM experiments. *Journal of Climate*, *13*(24), 4287–4309. https://doi.org/10.1175/1520-0442(2000)013<4287:IOEOTV>2.0.CO;2

Li, G., Xie, S.-P., & Du, Y. (2015). Climate model errors over the South Indian Ocean thermocline dome and their effect on the basin mode of interannual variability. *Journal of Climate*, *28*(8), 3093–3098. https://doi.org/10.1175/JCLI-D-14-00810.1

Lin, S., Dong, B., & Yang, S. (2024). Enhanced impacts of ENSO on the Southeast Asian summer monsoon under global warming and associated mechanisms. *Geophysical Research Letters*, *51*(2), e2023GL106437. https://doi.org/10.1029/2023GL106437

Liu, Y., & Chen, G. (2018). Intensified influence of the ENSO Modoki on boreal summer tropical cyclone genesis over the western North Pacific since the early 1990s. *International Journal of Climatology*, *38*(S1), e1258–e1265. https://doi.org/10.1002/joc.5347

Lu, T., Zhu, Z., Yang, Y., Ma, J., & Huang, G. (2023). Formation mechanism of the ENSO-independent summer western North Pacific anomalous anticyclone. *Journal of Climate*, *36*(6), 1711–1726. https://doi.org/10.1175/JCLI-D-22-0271.1

Masumoto, Y., & Meyers, G. (1998). Forced Rossby waves in the southern tropical Indian Ocean. *Journal of Geophysical Research*, *103*(C12), 27589–27602. https://doi.org/10.1029/98jc02546

Power, S. B., Delage, F., Colman, R., & Moise, A. (2012). Consensus on twenty-first-century rainfall projections in climate models more widespread than previously thought. *Journal of Climate*, *25*(11), 3792–3809. https://doi.org/10.1175/jcli-d-11-00354.1

Sharma, S., Ha, K.-J., Yamaguchi, R., Rodgers, K. B., Timmermann, A., & Chung, E.-S. (2023). Future Indian Ocean warming patterns. *Nature Communications*, *14*(1), 1789. https://doi.org/10.1038/s41467-023-37435-7

Song, F., & Zhou, T. (2015). The crucial role of internal variability in modulating the decadal variation of the East Asian summer Monsoon-ENSO relationship during the twentieth century. *Journal of Climate*, *28*(18), 7093–7107. https://doi.org/10.1175/jcli-d-14-00783.1

Tao, W. C., Huang, G., Hu, K. M., Qu, X., Wen, G. H., & Gong, H. N. (2015). Interdecadal modulation of ENSO teleconnections to the Indian Ocean basin mode and their relationship under global warming in CMIP5 models. *International Journal of Climatology*, *35*(3), 391–407. https://doi.org/10.1002/joc.3987

Taylor, K. E., Stouffer, R. J., & Meehl, G. A. (2012). An overview of CMIP5 and the experiment design. *Bulletin of the American Meteorological Society*, *93*(4), 485–498. https://doi.org/10.1175/bams-d-11-00094.1

Wang, B., Wu, R. G., & Fu, X. H. (2000). Pacific-East Asian teleconnection: How does ENSO affect East Asian climate? *Journal of Climate*, *13*, 1517–1536. https://doi.org/10.1175/1520-0442(2000)013<1517:PEATHD>2.0.CO;2

Wang, B., Wu, R. G., & Li, T. (2003). Atmosphere-warm ocean interaction and its impacts on Asian-Australian monsoon variation. *Journal of Climate*, *16*, 1195–1211. https://doi.org/10.1175/1520-0442(2003)16<1195:AOIAII>2.0.CO;2

Wang, B., Xiang, B. Q., & Lee, J. Y. (2013). Subtropical high predictability establishes a promising way for monsoon and tropical storm predictions. *Proceedings of the National Academy of Sciences of the United States of America*, *110*(8), 2718–2722. https://doi.org/10.1073/pnas.1214626110

Wang, G., Cai, W., & Santoso, A. (2020). Stronger increase in the frequency of extreme convective than extreme warm El Niño events under greenhouse warming. *Journal of Climate*, *33*(2), 675–690. https://doi.org/10.1175/jcli-d-19-0376.1

Wang, L., Chen, X., Zhao, Y., Zhou, T., Chen, L., & Sun, M. (2025). Enhanced trans-seasonal ENSO impact on East Asian-Western Pacific climate in warmer future: An emergent constraint from multi-large ensembles. *Geophysical Research Letters*, *52*(18), e2025GL116648. https://doi.org/10.1029/2025GL116648

Wu, B., Li, T., & Zhou, T. (2010). Relative contributions of the Indian Ocean and local SST anomalies to the maintenance of the Western North Pacific anomalous anticyclone during the El Niño decaying summer. *Journal of Climate*, *23*(11), 2974–2986. https://doi.org/10.1175/2010jcli3300.1

Wu, B., Zhou, T., & Li, T. (2017). Atmospheric dynamic and thermodynamic processes driving the Western North Pacific anomalous anticyclone during El Niño. Part II: Formation processes. *Journal of Climate*, *30*(23), 9637–9650. https://doi.org/10.1175/jcli-d-16-0495.1

Wu, M., Zhou, T., & Chen, X. (2021). The source of uncertainty in projecting the anomalous western North Pacific anticyclone during El Niño–decaying summers. *Journal of Climate*, 1–49. https://doi.org/10.1175/JCLI-D-20-0904.1

Wu, M., Zhou, T., Chen, X., & Wu, B. (2020). Intermodel uncertainty in the projection of the Anomalous Western North Pacific anticyclone associated with El Niño under global warming. *Geophysical Research Letters*, *47*(2), e2019GL086139. https://doi.org/10.1029/2019GL086139

Xie, S. P., Annamalai, H., Schott, F. A., & McCreary, J. P. (2002). Structure and mechanisms of South Indian Ocean climate variability. *Journal of Climate*, *15*(8), 864–878. https://doi.org/10.1175/1520-0442(2002)015<0864:SAMOSI>2.0.CO;2

Xie, S.-P., Hu, K., Hafner, J., Tokinaga, H., Du, Y., Huang, G., & Sampe, T. (2009). Indian Ocean capacitor effect on indo-western Pacific climate during the summer following El Niño. *Journal of Climate*, *22*(3), 730–747. https://doi.org/10.1175/2008jcli2544.1

Xie, S. P., Kosaka, Y., Du, Y., Hu, K. M., Chowdary, J., & Huang, G. (2016). Indo-western Pacific Ocean capacitor and coherent climate anomalies in post-ENSO summer: A review. *Advances in Atmospheric Sciences*, *33*(4), 411–432. https://doi.org/10.1007/s00376-015-5192-6

Yang, J. L., Liu, Q. Y., & Liu, Z. Y. (2010). Linking observations of the Asian monsoon to the Indian Ocean SST: Possible roles of Indian Ocean basin mode and dipole mode. *Journal of Climate*, *23*(21), 5889–5902. https://doi.org/10.1175/2010jcli2962.1

Yang, J. L., Liu, Q. Y., Xie, S. P., Liu, Z. Y., & Wu, L. X. (2007). Impact of the Indian Ocean SST basin mode on the Asian summer monsoon. *Geophysical Research Letters*, *34*(2), 5. https://doi.org/10.1029/2006gl028571

Zhang, R. H., Min, Q. Y., & Su, J. Z. (2017). Impact of El Niño on atmospheric circulations over East Asia and rainfall in China: Role of the anomalous western North Pacific anticyclone. *Science China Earth Sciences*, *60*(6), 1124–1132. https://doi.org/10.1007/s11430-016-9026-x

Zhang, R. H., & Sumi, A. (2002). Moisture circulation over East Asia during El Niño episode in northern winter, spring and autumn. *Journal of the Meteorological Society of Japan*, *80*(2), 213–227. https://doi.org/10.2151/jmsj.80.213

Zhang, R. H., Sumi, A., & Kimoto, M. (1996). Impact of El Niño on the East Asian monsoon: A diagnostic study of the '86/87 and '91/92 events. *Journal of the Meteorological Society of Japan*, *74*(1), 49–62. https://doi.org/10.2151/jmsj1965.74.1_49

Zhang, R. H., Sumi, A., & Kimoto, M. (1999). A diagnostic study of the impact of El Niño on the precipitation in China. *Advances in Atmospheric Sciences*, *16*(2), 229–241. https://doi.org/10.1007/bf02973084

Zhao, H., & Wang, C. (2019). On the relationship between ENSO and tropical cyclones in the western North Pacific during the boreal summer. *Climate Dynamics*, *52*(1–2), 275–288. https://doi.org/10.1007/s00382-018-4136-0

Zheng, X.-T., Gao, L., Li, G., & Du, Y. (2016). The southwest Indian Ocean thermocline dome in CMIP5 models: Historical simulation and future projection. *Advances in Atmospheric Sciences*, *33*(4), 489–503. https://doi.org/10.1007/s00376-015-5076-9

Zheng, X.-T., Xie, S.-P., & Liu, Q. (2011). Response of the Indian Ocean basin mode and its capacitor effect to global warming. *Journal of Climate*, *24*(23), 6146–6164. https://doi.org/10.1175/2011jcli4169.1